The effect of external forces on discrete motion within holographic optical tweezers

E. Eriksson[1,2], S. Keen[2], J. Leach[2], M. Goksör[1,2*] and M. J. Padgett[2*]

[1]*Department of Physics, Göteborg University, SE-41296 Göteborg, Sweden*
[2]*SUPA, Physics and Astronomy, Kelvin Building, University of Glasgow, Glasgow G12 8QQ.*

mattias.goksor@physics.gu.se

m.padgett@physics.gla.ac.uk

Abstract: Holographic optical tweezers is a widely used technique to manipulate the individual positions of optically trapped micron-sized particles in a sample. The trap positions are changed by updating the holographic image displayed on a spatial light modulator. The updating process takes a finite time, resulting in a temporary decrease of the intensity, and thus the stiffness, of the optical trap. We have investigated this change in trap stiffness during the updating process by studying the motion of an optically trapped particle in a fluid flow. We found a highly nonlinear behavior of the change in trap stiffness vs. changes in step size. For step sizes up to approximately 300 nm the trap stiffness is decreasing. Above 300 nm the change in trap stiffness remains constant for all step sizes up to one particle radius. This information is crucial for optical force measurements using holographic optical tweezers.

OCIS codes: (090.2890) Holographic optical elements; (140.7010) Laser trapping; (170.4520) Optical confinement and manipulation

References and links

1. A. Ashkin, J. M. Dziedzic, J. E. Bjorkholm, and S. Chu, "Observation of a single-beam gradient force optical trap for dielectric particles," Opt. Lett. **11**, 288–290 (1986).
2. J. E. Molloy and M. J. Padgett, "Lights, action: optical tweezers," Contemp. Phys. **43**, 241–258 (2002).
3. D. McGloin, "Optical tweezers: 20 years on," Philos. T. R. Soc. A **364**, 3521–3537 (2006).
4. K. Svoboda and S. M. Block, "Biological applications of optical forces," Annu. Rev. Bioph. Biom. **23**, 247–285 (1994).
5. R. M. Simmons, J. T. Finer, S. Chu, and J. A. Spudich, "Quantitative measurements of force and displacement using an optical trap," Biophys. J. **70**, 1813–1822 (1996).
6. J. C. Meiners and S. R. Quake, "Femtonewton force spectroscopy of single extended DNA molecules," Phys. Rev. Lett. **84**, 5014–5017 (2000).
7. J. Liesener, M. Reicherter, T. Haist, and H. J. Tiziani, "Multi-functional optical tweezers using computer-generated holograms," Opt. Commun. **185**, 77–82 (2000).
8. J. E. Curtis, B. A. Koss, and D. G. Grier, "Dynamic holographic optical tweezers," Opt. Commun. **207**, 169–175 (2002).
9. P. Jordan, J. Leach, M. Padgett, P. Blackburn, N. Isaacs, M. Goksor, D. Hanstorp, A. Wright, J. Girkin, and J. Cooper, "Creating permanent 3D arrangements of isolated cells using holographic optical tweezers," Lab Chip **5**, 1224–1228 (2005).
10. G. M. Akselrod, W. Timp, U. Mirsaidov, Q. Zhao, C. Li, R. Timp, K. Timp, P. Matsudaira, and G. Timp, "Laser-guided assembly of heterotypic three-dimensional living cell microarrays," Biophys. J. **91**, 3465–3473 (2006).
11. R. Di Leonardo, J. Leach, H. Mushfique, J. M. Cooper, G. Ruocco, and M. J. Padgett, "Multipoint holographic optical velocimetry in microfluidic systems," Phys. Rev. Lett. **96**, 134502 (2006).

#88373 - $15.00 USD Received 8 Oct 2007; revised 14 Dec 2007; accepted 14 Dec 2007; published 20 Dec 2007

12. E. Eriksson, J. Enger, B. Nordlander, N. Erjavec, K. Ramser, M. Goksor, S. Hohmann, T. Nystrom, and D. Hanstorp, "A microfluidic system in combination with optical tweezers for analyzing rapid and reversible cytological alterations in single cells upon environmental changes," Lab Chip **7**, 71–76 (2007).
13. E. Eriksson, J. Scrimgeour, J. Enger, and M. Goksor, "Holographic optical tweezers combined with a microfluidic device for exposing cells to fast environmental changes," Proc. SPIE **6592**, 65920P-9 (2007).
14. M. Reicherter, S. Zwick, T. Haist, C. Kohler, H. Tiziani, and W. Osten, "Fast digital hologram generation and adaptive force measurement in liquid-crystal-display-based holographic tweezers," Appl. Opt. **45**, 888–896 (2006).
15. C. H. J. Schmitz, J. P. Spatz, and J. E. Curtis, "High-precision steering of multiple holographic optical traps," Opt. Express **13**, 8678–8685 (2005).
16. S. Keen, J. Leach, G. Gibson, and M. Padgett, "Comparison of a high-speed camera and a quadrant detector for measuring displacements in optical tweezers," J. Opt. A-Pure Appl. Opt. **9**, S264–S266 (2007).
17. A. Ashkin, "Forces of a single-beam gradient laser trap on a dielectric sphere in the ray optics regime," Biophys. J. **61**, 569–582 (1992).

1. Introduction

Optical tweezers [1] have become a useful tool for manipulating micron-sized particles and cells [2, 3]. For small displacements of an optically trapped object the restoring optical gradient force scales linearly with the distance from the trap center. This enables investigations of forces in the femto- and pico-Newton regime [4, 5, 6].

In the late 1990s optical tweezers were developed further by the implementation of spatial light modulators (SLMs) placed in the Fourier plane of the trapping plane. A single optical trap could thus be divided into several optical traps, each individually controllable by updating the kinoform displayed on the SLM [7, 8]. The SLMs used for optical tweezers applications are commonly based on liquid crystals that modulate the phase of the incident light. The diffraction efficiency of liquid crystal SLMs is high due to the many addressable phase levels. However, a limitation is the slow response time of the liquid crystal.

Holographic optical tweezers (HOT) has recently found its applications in life science where parallel single cells in an array can be manipulated and studied simultaneously [9, 10]. In combination with microfluidic systems, HOT offers several new possibilities for flow measurement [11] and the ability to control the local environment of single cells in parallel [12, 13]. HOT have also been used for optical force measurement (OFM) applications [14]. HOT thus allow OFM to be performed with several trapped particles simultaneously. OFM either keeps the trap position fixed and measures the displacement of the trapped object from the trap center, or uses the positional data to continuously adjust the trap position to bring the particle back to its initial position. The later "closed loop" configuration allows a true force measurement to be performed, but requires the ability to rapidly and continuously adjust the trap position. In most closed-loop configurations the trap movement is achieved using acousto-optic deflectors (AOD).

The minimum update of the step size possible with HOT is in the sub-nanometer range [15]. In principle it is therefore possible to move optically trapped particles with HOT in a close to continuous fashion. However, the update frequency of the SLM is, beside the technical aspects, limited by the computation time required to calculate the required kinoforms. In practice the movement of trapped objects is restricted to discrete steps. In this paper we study the movement of optically trapped particles by HOT in a fluid flow during the SLM update for various step sizes. As the SLM momentarily divert lights away from the intended traps during the update process, it causes a temporary weakening of the trap stiffness. This is crucial for OFM applications, where it is important to have control of the trap stiffness. The weakening of the trap stiffness is here quantified and used to establish operating guidelines by which the performance of HOT for OFM and/or microfluidics applications can be optimized.

#88373 - $15.00 USD Received 8 Oct 2007; revised 14 Dec 2007; accepted 14 Dec 2007; published 20 Dec 2007

2. Experimental procedure

The experimental setup is illustrated in Fig. 1. The HOT setup is configured around an inverted Zeiss Axiovert 200 microscope with a 1.3NA,100×, Plan Neo-fluar objective. The optical traps were created using a 1.5 W, 532 nm cw laser. The laser beam was expanded to slightly overfill the SLM (Hamamatsu X8267, 768×768 pixels, 20×20 mm^2, 256 phase levels), which was imaged onto the back aperture of the microscope objective. The kinoforms were calculated as blazed gratings to give an angular displacement of the diffracted beam and hence a lateral displacement of the trap [14].

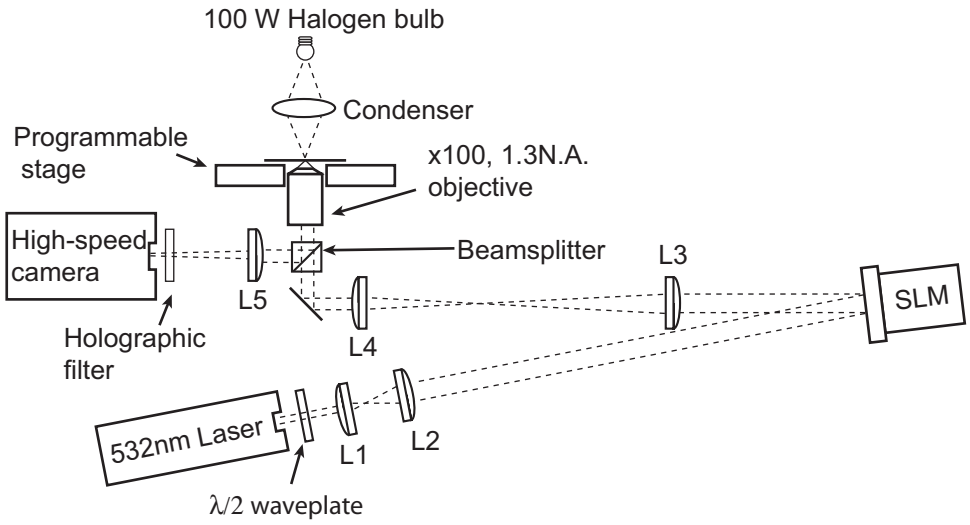

Fig. 1. A schematic drawing of the experimental setup used to measure the position of a trapped particle in a fluid flow. The laser beam was expanded (lenses L1 and L2, focal lengths $f_1 = 30$ mm and $f_2 = 200$ mm) to slightly overfill the SLM. A $\lambda/2$ plate was used to adjust the polarization direction of the laser to that of the SLM. The size of the beam reflected off the SLM was then reduced to fit the size of the back aperture of the microscope objective (lenses L3 and L4, focal lengths $f_3 = 600$ mm and $f_4 = 200$ mm) that focussed the light to form the optical traps.

All experiments were performed with a single silica bead trapped 10 μm away from the zeroth order optical trap and 5 μm from the coverslip. The particle was stepped in a direction perpendicular to a fluid flow, as illustrated in Fig. 2. The flow was created by translating the microscope stage with a uniform speed back and forth over a distance of 500 μm. The Stokes drag force of a trapped particle of radius r, generated by a fluid flow of velocity v and viscosity η is given by $F = 6\pi r v \eta$.

A halogen 100 W light bulb and a 0.8NA condenser was used to illuminate the sample, which was imaged using a CMOS camera mounted on the viewing port of the microscope. When used at its full 1280×1024 resolution the CMOS sensor has a standard video frame rate of 24 Hz. However, by reducing the region of interest (ROI) the frame rate could be increased. For the measurements on 1.1 μm and 2.0 μm diameter beads the ROI was reduced to allow images to be taken at 1 kHz, while the larger 5.0 μm beads were imaged at 500 Hz. The scale of the image was calibrated against an object micrometer. The position of the trapped bead was measured while stepping the trapped particle during 50 s (1.1 μm and 2.0 μm beads) or 60 s (5.0 μm beads) using a real-time, center-of-mass tracking algorithm with an accuracy in the order of 10 nm [16]. The positional data was then analyzed to extract information about

#88373 - $15.00 USD Received 8 Oct 2007; revised 14 Dec 2007; accepted 14 Dec 2007; published 20 Dec 2007

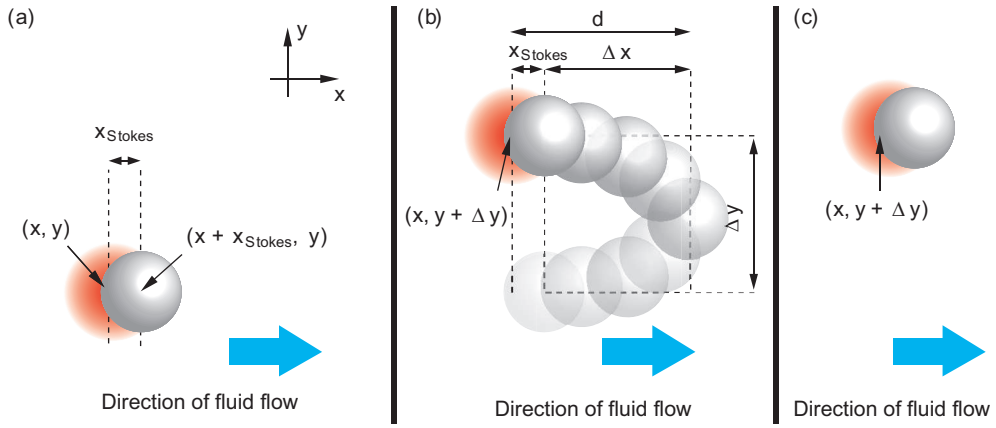

Fig. 2. An illustration of using HOT to move a particle from position (x,y) to position $(x,y+\Delta y)$ in the presence of flow in the x-direction. (a) The initial position of the optical trap is at (x,y). (b) The location of the optical trap is updated to $(x,y+\Delta y)$ and the maximum downstream displacement, Δx, as a function of the step size, Δy, is measured. (c) The bead trapped at the new location.

the maximum downstream displacement, Δx, during each hologram update and the steady state downstream displacement due to Stokes drag, x_{Stokes} (c.f. Fig. 2). The trap position was updated at 0.5 Hz, resulting in approximately 25 measurements of Δx for the smaller particles (1.1 μm and 2.0 μm) and 30 measurements for the larger particle (5.0 μm) for each step size. The measured downstream displacements were averaged to give one data point for each step size and particle size.

3. Results and discussion

A typical example of the experimental data is shown in Fig. 3. For ease of illustration only 6 seconds of data are shown, 2 seconds in each of the 3 trap positions. In these plots it is possible to distinguish all the key parameters, including the steady state downstream displacement due to the Stokes drag force acting on the trapped particle (x_{Stokes}), the residual Brownian motion, the HOT step size (Δy) and the inter-step downstream displacement (Δx) that occurs while the hologram is being updated on the SLM.

In this study we have focused on the inter-step downstream displacement relative to the center of the trap, $d = x_{Stokes} + \Delta x$, as a function of particle size and step size. The experimental data of the measured total displacements, d, during the SLM update are shown for three different particle sizes as a function of step size in Fig. 4. The behavior is essentially the same for all three bead sizes. The downstream displacement increases with step size up to 200-300 nm after which it becomes constant for step sizes up to one particle radius. For step sizes above one particle radius the downstream displacement increases again.

To explain this non-linear behavior it is necessary to look at the intensity in the optical trap while updating the SLM with a kinoform corresponding to the new trap position. Such an intensity measurement is shown in Fig. 5(a), where the intensity of the laser light reflected off the coverslip was monitored with a CMOS camera in a ROI containing both trap positions. The intensity measurement confirms that light is diverted away from the optical trap during the time the SLM is updating the hologram. This "dead time" was on the order of 200 ms, which is also in agreement with the SLM specifications. The dead time was found to be constant regardless

#88373 - $15.00 USD Received 8 Oct 2007; revised 14 Dec 2007; accepted 14 Dec 2007; published 20 Dec 2007

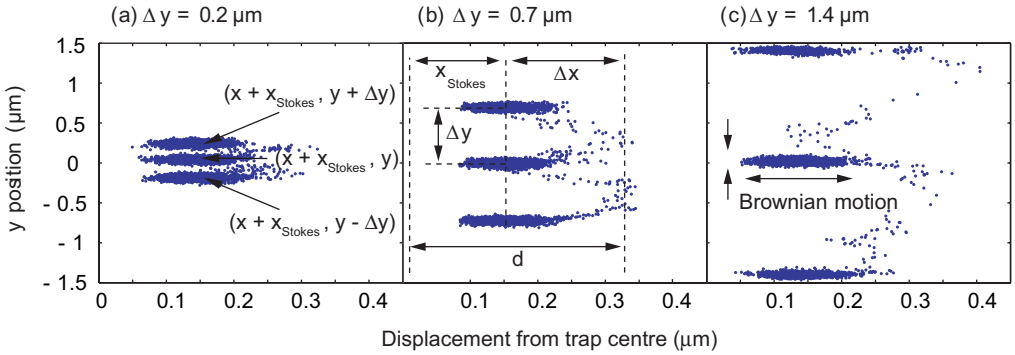

Fig. 3. Positional data for a bead (2 μm in diameter) trapped in a 50 μm/s flow illustrated as *xy* scatter plots. Data for $\Delta y = \pm 0.2, 0.7, 1.4$ μm is shown in (a), (b) and (c) respectively. The particle is moved from top to bottom in all of the figures. Note that the displacement due to Stokes drag force, x_{Stokes}, can be seen. The aspect ratio of this diagram has been set to 7:1 in order to emphasize Δx.

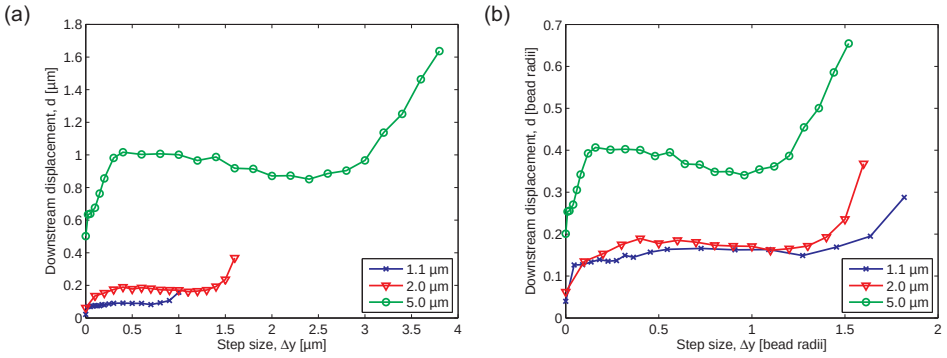

Fig. 4. The measured downstream displacement, $d = x_{Stokes} + \Delta x$, as a function of step size for 1.1, 2.0 and 5.0 μm diameter particles, subject to a perpendicular fluid flow of 50 μm/s. (a) Distances measured in micrometer and (b) distances normalized to particle radii.

of the trap step size, whereas the intensity loss was measured to be dependent on step size (c.f. Fig. 5(b), left axis). The intensity loss increased up to a step size of 300 nm, after which the intensity loss remained constant. This also explains why the downstream drag increases for step sizes up to 200-300 nm.

Further, the behavior of the intensity can be explained from the calculated kinoforms as the step sizes increases (the holograms are assumed to have phase values between 0 and 2π, scaling linearly with the digital signal sent to the SLM). In Fig. 5(b) (blue curve, right axis) the average phase shift per pixel when taking steps of various sizes is shown (steps are in the positive *y* direction, starting at $x = 10$ μm, $y = 0$ μm). Since the amplitude profile of the incident beam falling onto the SLM is Gaussian shaped, pixels in the center of the SLM affect the trap intensity more than pixels on the border of the SLM. Therefore, the phase change values for different pixels have been weighted with a Gaussian with a width matched to the size of the SLM before calculating the average phase change per pixel. The calculated average phase shift per pixel increases for step sizes up to 200 nm (in our setup corresponding to 1.6 grating periods across the SLM), which is in good agreement with both the intensity measurements

#88373 - $15.00 USD Received 8 Oct 2007; revised 14 Dec 2007; accepted 14 Dec 2007; published 20 Dec 2007

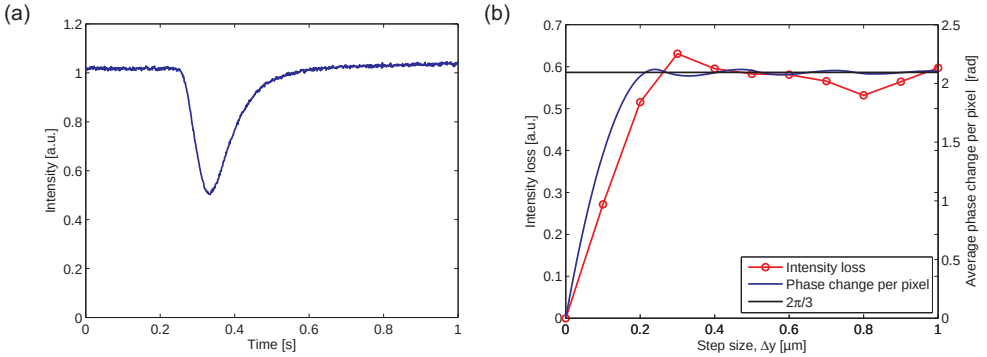

Fig. 5. (a) The measured intensity reflected off the coverslip as the SLM was updated from one hologram to another. While the SLM is updating the hologram, light is diverted away from the trapping region, thus decreasing the measured intensity. The intensity was measured in a region of interest containing both traps, when moving from $x = 10$ μm, $y = 0$ μm to $x = 10$ μm, $y = 0.2$ μm in one step. (b) Left axis (red curve): the dependence of the depth of the intensity decrease on step size (steps are in the positive y direction, starting at $x = 10$ μm, $y = 0$ μm). Right axis (blue curve): The average phase change per pixel between two kinoforms as a function of step size (steps are in the positive y direction, starting at $x = 10\mu$m, $y = 0\mu$m), weighted with a Gaussian intensity profile. The curve saturates at a phase shift of $2\pi/3$ (black line).

and the measurements of the downstream displacement. It can also be noted that the average phase shift per pixel approaches $2\pi/3$ for large step sizes. This situation is equivalent to the average phase shift per pixel when changing from an arbitrary blazed grating to a hologram with a constant phase level, where the constant phase level corresponds to the RMS value of a flat probability distribution of phase values between 0 and 2π. This explanation was further supported by measuring the downstream displacements when adding a constant phase shift per pixel to the hologram (without moving the trap position). For a range of fluid flow rates the downstream displacements for an average phase shift per pixel of $2\pi/3$ agreed well with the downstream displacements found for step sizes in the range of 300 nm up to one particle radius (see Fig. 6). As expected from the Stokes drag force, there is a linear dependence of the downstream displacement as a function of flow rate.

The increasing downstream displacement for step sizes above one particle radius is perhaps the most intuitive part of the experimental data. The force acting on a particle is well known to fall off rapidly once the particle is more than one particle radius away from the center of the trap [17].

It is worth noting that the scaling between the change in grating period of the displayed holograms and the step size in the trapping plane will differ between different optical setups. The scaling depends mainly on the wavelength, the effective focal length of the microscope objective and the magnification of the imaging optics between the SLM and the microscope objective. Another important parameter that will differ between HOT setups is the response time of the SLM, which will affect the magnitude of the downstream displacement.

4. Conclusions

When using SLMs for HOT applications one critical question is what step size that should be used during particle movement. The movement of the optically trapped particle should be both rapid but not likely to result in an escaped particle. For optical force measurement applications

#88373 - $15.00 USD Received 8 Oct 2007; revised 14 Dec 2007; accepted 14 Dec 2007; published 20 Dec 2007

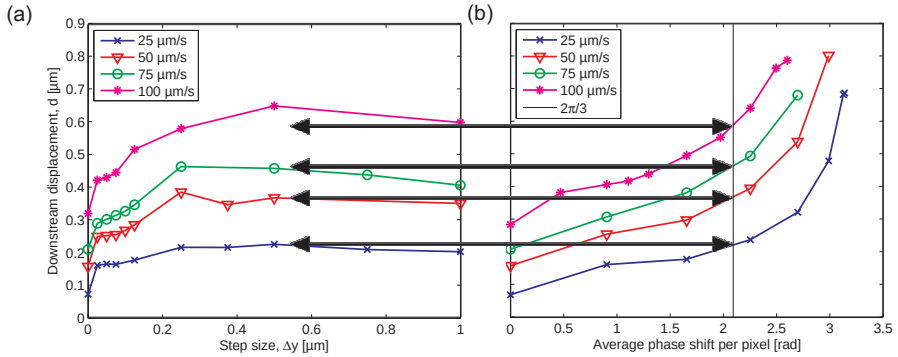

Fig. 6. Measured total downstream displacement, $d = x_{Stokes} + \Delta x$, for four different flow rates: 25, 50, 75 and 100 μm/s. The measurements were done with a 2.0 μm diameter particle trapped with approximately 12 mW of laser power. In figure (a) the step size was varied and in figure (b) a phase change was added to the trapping hologram (without updating trap position). Note that the downstream displacements for an average phase shift per pixel of $2\pi/3$ agrees well with with the downstream displacements found for step sizes in the range 300 nm up to one particle radius.

it is also very important to know the stiffness of the optical trap (and preferably to keep it constant). By measuring the downstream displacement in a fluid flow due to the decrease in trap stiffness during the update of the SLM (Hamamatsu X8267) we have identified some general guidelines for HOT using a phase-only SLM with a range of 2π:

First, for step sizes above the particle radius the downstream displacement during the SLM update increases dramatically, since the restoring force of the optical trap falls off quickly outside one particle radius.

Secondly, for step sizes between 300 nm (corresponding to 2.3 grating periods across the SLM) and one particle radius, the inter-step downstream displacement is approximately independent of step size. This can be explained by the decrease in trap intensity during the SLM update, which is constant in this range. The constant intensity loss is due to a roughly constant average hologram phase shift per pixel. The data also demonstrates that the time needed for the trapped particle to travel to the new position is negligible compared to the updating time of the SLM. In addition, the downstream displacement is proportional to the fluid flow rate, as expected from the Stokes drag force acting on the particle.

Finally, for step sizes up to 300 nm, the inter-step downstream displacement is increasing. In this range the average phase shift per pixel in the holograms is increasing with the hologram step size, resulting in an increasing intensity loss during the SLM update.

In conclusion, in applications where a quick movement of the trap is desired and a decrease in trap stiffness is tolerated, it is beneficial to move the trap with steps equalling the bead/cell radius. On the other hand, in applications where it is crucial to keep an almost constant trap stiffness, the trap should be moved in as small steps as allowed by the HOT setup.

Acknowledgments

This work was funded by the Carl Trygger Foundation for Scientific Research (MG).

#88373 - $15.00 USD Received 8 Oct 2007; revised 14 Dec 2007; accepted 14 Dec 2007; published 20 Dec 2007